



This is a repository copy of *Experimental and modelling study of hydrogen ignition in CO<sub>2</sub> bath gas*.

White Rose Research Online URL for this paper:

<https://eprints.whiterose.ac.uk/190074/>

Version: Submitted Version

---

**Preprint:**

Harman-Thomas, J.M., Kashif, T.A., Hughes, K.J. orcid.org/0000-0002-5273-6998 et al. (2 more authors) (Submitted: 2022) Experimental and modelling study of hydrogen ignition in CO<sub>2</sub> bath gas. [Preprint]

<https://doi.org/10.2139/ssrn.4172054>

---

© 2022 The Author(s). This is an author-produced version of a paper subsequently submitted to SSRN. For re-use permissions please contact the author(s).

**Reuse**

Items deposited in White Rose Research Online are protected by copyright, with all rights reserved unless indicated otherwise. They may be downloaded and/or printed for private study, or other acts as permitted by national copyright laws. The publisher or other rights holders may allow further reproduction and re-use of the full text version. This is indicated by the licence information on the White Rose Research Online record for the item.

**Takedown**

If you consider content in White Rose Research Online to be in breach of UK law, please notify us by emailing [eprints@whiterose.ac.uk](mailto:eprints@whiterose.ac.uk) including the URL of the record and the reason for the withdrawal request.



[eprints@whiterose.ac.uk](mailto:eprints@whiterose.ac.uk)  
<https://eprints.whiterose.ac.uk/>

# Experimental and Modelling Study of Hydrogen Ignition in CO<sub>2</sub> Bath Gas

James M. Harman-Thomas<sup>1,+</sup>, Touqeer Anwar Kashif<sup>2,+</sup>, Kevin J. Hughes<sup>1</sup>, Mohamed Pourkashanian<sup>1</sup>,  
Aamir Farooq<sup>2,\*</sup>

<sup>1</sup>The University of Sheffield, Department of Mechanical Engineering, Energy 2050, Sheffield, United Kingdom

<sup>2</sup>Clean Combustion Research Center, King Abdullah University of Science and Technology (KAUST), Thuwal  
23955, Saudi Arabia

\*Corresponding author email: [aamir.farooq@kaust.edu.sa](mailto:aamir.farooq@kaust.edu.sa)

+Both Authors Contributed Equally

## Abstract

Direct-fired supercritical CO<sub>2</sub> power cycles, operating on natural gas or syngas, have been proposed as future energy technologies with 100% carbon capture at a price competitive with existing fossil fuel technologies. Likewise, blue or green hydrogen may be used for power generation to counter the intermittency of renewable power technologies. In this work, ignition delay times (IDTs) of hydrogen were measured in a high concentration of CO<sub>2</sub> bath gas over 1050 – 1300 K and pressures between 20 and 40 bar. Measured datasets were compared with chemical kinetic simulations using AramcoMech 2.0 and the University of Sheffield supercritical CO<sub>2</sub> (UoS sCO<sub>2</sub> 2.0) chemical kinetic mechanisms. The UoS sCO<sub>2</sub> 2.0 mechanism was recently developed to model IDTs of methane, hydrogen, and syngas in CO<sub>2</sub> bath gas. Sensitivity analyses were used to identify important reactions and to illustrate the trends observed among various datasets. The performance of both mechanisms was evaluated quantitatively by comparing the average absolute error between the predicted and experimental IDTs, which showed UoS sCO<sub>2</sub> 2.0 as the superior mechanism for modelling hydrogen IDTs in CO<sub>2</sub> bath gas. The importance of OH time-histories is identified as the most appropriate next step in further validation of the kinetic mechanism.

**Keywords:** *Supercritical CO<sub>2</sub>; Hydrogen; Ignition Delay Time; Shock Tube; Chemical Kinetics*

## 1        **1. Introduction**

2        The IPCC's Sixth Assessment Report (2021) revealed that anthropogenic activities have caused a global  
3        surface temperature rise of 1.07 °C from 1850-1900 to 2010-2019 [1]. The increase in global temperatures  
4        and the resulting climate change has led to an increase in the frequency and intensity of extreme weather  
5        events worldwide. In 2019 alone, there were 396 global disasters worldwide, affecting 95 million people  
6        and costing nearly US\$130 billion [2]. As of 2021, 131 countries have announced or adopted policies to  
7        become net-zero by 2060 or earlier [3]. However, it is extremely unlikely that our reliance on fossil fuels  
8        will disappear anytime soon, implying that methods of utilizing fossil fuels without releasing harmful  
9        emissions into the atmosphere will be required to meet these targets.

10        Direct-fired supercritical CO<sub>2</sub> (sCO<sub>2</sub>) combustion cycles have the potential for 100% inherent carbon  
11        capture at a price competitive with existing fossil fuel technology [4]. Direct-fired sCO<sub>2</sub> cycles operate  
12        above 300 atm with a 96% dilution of carbon dioxide (CO<sub>2</sub>), above its critical pressure and temperature,  
13        where it becomes supercritical and possesses properties of both a liquid and a gas [4]. The Allam-Fetvedt  
14        cycle is the most established direct-fired sCO<sub>2</sub> cycle, with an operational 50 MW pilot plant [5], and two  
15        280 MW plants in the US and one 300 MW plant under development in the UK [6, 7]. The combustion  
16        chamber of the Allam-Fetvedt cycle has a predicted generation efficiency of 53.9% for natural gas  
17        combustion [8]. Burning natural gas and pure oxygen, produced from an onsite air separation unit,  
18        produces water and CO<sub>2</sub> as the only products of combustion. These can be easily separated via the  
19        condensation of water to produce a high-purity stream of CO<sub>2</sub> which can be sequestered or used in various  
20        chemical conversion processes.

21        One current challenge faced by the Allam-Fetvedt cycle is the lack of a reliable chemical kinetic  
22        mechanism that can accurately model combustion at high pressures with a large dilution of CO<sub>2</sub>. Most of  
23        the available experimental data have been measured at lower pressures and with a smaller mole fraction  
24        of CO<sub>2</sub>. Recently, the University of Sheffield Supercritical CO<sub>2</sub> Mechanism (UoS sCO<sub>2</sub> Mech) [9] was

25 developed using literature ignition delay time (IDT) data of methane, hydrogen (H<sub>2</sub>) and syngas over a  
26 range of pressures and CO<sub>2</sub> dilutions. This work identified a need for further H<sub>2</sub> IDT measurements as few  
27 (only three) datasets are available at relevant conditions. Shao et al. [10] studied IDTs of H<sub>2</sub> with 85%  
28 CO<sub>2</sub> dilution at approximately 38, 110 and 271 bar. Interestingly, the investigated chemical kinetic  
29 mechanisms showed a better agreement with the higher pressure datasets than at 38 bar [11]. Therefore,  
30 IDT data between 20 and 40 bar at various equivalence ratios and CO<sub>2</sub> dilutions are needed to validate  
31 and improve the performance of chemical kinetics mechanisms at these conditions.

32 The current work is aimed at obtaining new IDT data for H<sub>2</sub> ignition in a high concentration of CO<sub>2</sub>  
33 bath gas. Ignition delays were measured at high temperatures and 20-40 bar pressures with variable bath  
34 gas compositions (N<sub>2</sub>, CO<sub>2</sub>). The datasets were subsequently compared with predictions of UoS sCO<sub>2</sub>  
35 Mech and AramcoMech 2.0 to evaluate their performance in modelling CO<sub>2</sub>-diluted H<sub>2</sub> ignition.

## 36 **2. Experimental Details**

37 Ignition delays of hydrogen were measured in the high-pressure shock tube (HPST) facility at King  
38 Abdullah University of Science and Technology (KAUST). The HPST is constructed from stainless steel  
39 capable of withstanding pressures up to 300 bar. The driven section is 6.6 m long with a circular cross-  
40 sectional diameter of 10.16 cm. The driver section is modular and can be extended up to 6.6 m. It houses  
41 a double diaphragm arrangement which allows for better shock-to-shock repeatability. Further details of  
42 the facility may be found elsewhere [12-14].

43 Incident shock speed was measured by six PCB 113B26 piezoelectric pressure transducers (PZTs),  
44 placed axially along the last 3.6 m of the driven section. Rankine-Hugnoit shock relations were used to  
45 calculate thermodynamic conditions (P<sub>5</sub> and T<sub>5</sub>) behind reflected shock waves with uncertainties of <1%.  
46 Incident shock attenuation rates varied from 0.5 to 1.8%/m.

47

48

49 **Table 1.** IDT mixtures studied in this work and the results of quantitative comparisons.

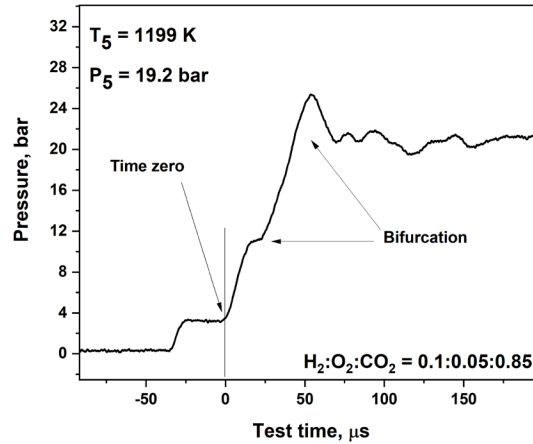
Mix.	Species Mole Fraction				Mixture Conditions			Average Absolute Error ( $E$ ) (%)	
	H <sub>2</sub>	O <sub>2</sub>	N <sub>2</sub>	CO <sub>2</sub>	T [K]	P [bar]	$\phi$	AramcoMech 2.0	UoS sCO <sub>2</sub> 2.0
1	10	5	35	50	1103- 1243	20.5- 21.7	1.0	40.9	3.1
2	10	5	-	85	1142- 1261	18.5- 19.6	1.0	50.0	11.8
3	10	5	85	-	1059- 1214	19.2- 20.5	1.0	13.6	18.2
4	12	3	35	50	1123- 1238	20.2- 21.0	2.0	11.4	22.4
5	4.3	10.7	35	50	1162- 1255	19.4- 19.9	0.2	59.5	29.0
6	5	10	-	85	1204- 1302	42.0- 43.0	0.25	17.0	14.4
7	7.5	7.5	-	85	1164- 1300	41.4- 42.1	0.5	7.8	18.1
8	10	5	-	85	1123- 1266	40.5- 41.6	1.0	24.4	11.6
<b>Average <math>E</math> (%)</b>								28.1	16.1

50 Sidewall pressure was monitored using a Kistler 603B1 PZT and OH\* chemiluminescence signals were  
51 measured at the endwall and sidewall through photomultiplier tubes (PMTs). Mixtures were prepared in  
52 a 20 L stainless steel vessel equipped with a magnetic stirrer. Research grade (99.999%) gases were used,  
53 and each mixture was given sufficient time to mix before experiments to ensure homogeneity. Table 1  
54 shows the compositions of the 8 mixtures investigated along with the reflected-shock temperature and  
55 pressure ranges. These mixture compositions were selected to fill in the gaps in literature IDT datasets of  
56 hydrogen over 20 – 40 bar and to investigate the effect of varying CO<sub>2</sub> bath gas composition equivalence  
57 ratio. A kinetic mechanism should be able to accurately simulate combustion at lower pressures before  
58 expanding to the higher pressures of the Allam-Fetvedt cycle.

### 59 2.1. Identification of Time Zero

60 Time zero identification is challenging for mixtures with high levels of CO<sub>2</sub> dilution, as has been reported  
61 in literature shock tube studies [15, 16]. Non-idealities from CO<sub>2</sub> dilution mainly originate due to the  
62 interaction of the reflected shock wave (RSW) with an energy-deficient boundary layer behind the incident  
63 shock wave (ISW), thus leading to the bifurcation of the reflected shock. An oblique shock will then

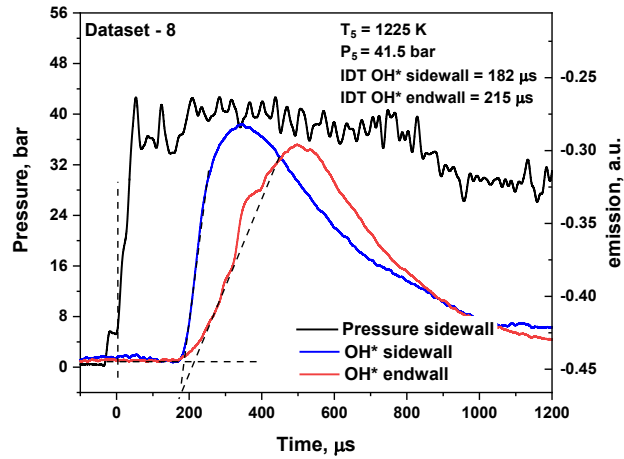
64 precede the normal shock near the boundaries, thus altering the state of gas in region 5 (i.e., behind the  
65 RSW) [17-19]. These alterations are more pronounced in regions further from the endwall. Such fluid  
66 disturbances manifest themselves in the pressure profiles at endwall and sidewall transducers.



67

68 Fig. 1. Sidewall pressure history for a representative experiment of 85% CO<sub>2</sub> diluted H<sub>2</sub> mixture.

69 Hargis et al. [15] compared sidewall and endwall pressure histories at various CO<sub>2</sub> dilutions for methane  
70 mixtures, and highlighted the superiority of endwall pressure profiles for time zero determination. Due to  
71 the lack of an endwall pressure transducer in the present work, measurements were made with a sidewall  
72 Kistler transducer located just 10.48 mm from the endwall. In contrast to the usual practice where time  
73 zero is defined as the midpoint of the reflected shock wave, time zero is defined in this work at the start  
74 of reflected shock pressure rise. This is based on inferences from the pressure traces of Hargis et al. [15]  
75 and Karimi et al. [16]. Figure 1 shows a representative sidewall pressure trace for an 85% CO<sub>2</sub>-diluted H<sub>2</sub>  
76 mixture at 20 bar from the present work. The extent of bifurcation is significantly smaller than in Hargis  
77 et al. [15] experiments, and this is likely due to their sidewall pressure transducer being further away (16  
78 mm) from the endwall.



79

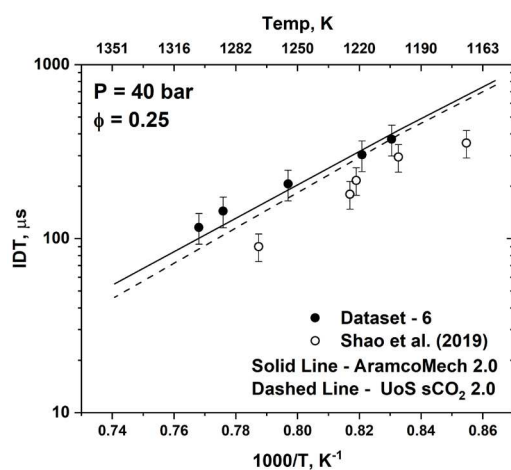
80 Fig. 2. Representative profiles for IDT measurements of dataset 8 ( $\text{H}_2:\text{O}_2:\text{CO}_2=10:5:85$ ) at 1225 K.

81 **2.2. Determination of Ignition Delay**

82 In an ideal scenario with a homogenous temperature and pressure field behind the reflected shock wave,  
 83 the mixture is expected to ignite near the endwall as the gas there is exposed to high-temperature  
 84 conditions for a longer duration compared to the gas further away from the endwall. The onset of ignition  
 85 is then determined through the steep rise in endwall/sidewall pressure or OH\*. These methods give very  
 86 similar IDTs in ideal conditions [20].

87 At high levels of  $\text{CO}_2$  dilution, small hot spots can develop as a result of interactions between the RSW  
 88 and the boundary layer [21]. These hot spots alter the homogeneity of the mixture and can potentially  
 89 cause an early initiation of the ignition process which can lead to a false interpretation of IDTs from  
 90 pressure and emission traces. For the present mixtures, a noticeable early rise of OH\* sidewall emission  
 91 was observed, as can be seen in Fig. 2. Similar observations were reported by Karimi et al. [16] for heavily  
 92 diluted  $\text{CO}_2$  mixtures. They associated the hotspots formed in the periphery of the shock tube to the  
 93 increased bifurcation in these mixtures. The small ignition kernels are picked up by the sidewall OH\*  
 94 earlier than the endwall emission. The large internal diameter of the shock tube ensures that the core of  
 95 the mixture remains unaffected, as reported by Karimi et al. [16]. Endwall emission thus responds to the  
 96 ignition of the core gas as it sees the bulk of the volume [20].

97 Therefore, in this work, the onset of ignition was determined through the maximum slope of the OH\*  
 98 endwall emission trace. A comparison of IDTs for H<sub>2</sub> dataset 6 (5% H<sub>2</sub>/10% O<sub>2</sub>/ 85% CO<sub>2</sub>) against a  
 99 dataset from Shao et al. [10] is shown in Fig. 3. The two datasets are in relatively good agreement at lower  
 100 temperatures. The disagreement in the datasets at a higher temperature may be explained by the high  
 101 uncertainty of IDTs smaller than 100 μs due to the uncertainty in identifying time zero. The discrepancy  
 102 seen between the present data and that of Shao et al. [10] is likely down to the different methods of IDT  
 103 determination. Shao et al. [10] used sidewall emissions, which as discussed, is more sensitive to the early-  
 104 onset ignition, explaining the smaller value of their measured IDT compared to the endwall IDT from the  
 105 present study. Uncertainty in our measured ignition delay times is estimated to be +/- 20% (see  
 106 Supplementary Material).



107  
 108 Fig. 3. Comparison of mixture 6 (H<sub>2</sub>:O<sub>2</sub>:CO<sub>2</sub>=5:10:85) IDTs with literature data [10].

### 109 3. Modelling Procedure

110 IDTs were modelled using Chemkin-Pro (zero-D batch reactor, constant UV) with two chemical kinetic  
 111 mechanisms, namely AramcoMech 2.0 [22] and UoS sCO<sub>2</sub> 2.0 [9, 11]. A 2.5%/ms dp/dt was incorporated  
 112 in the simulations to account for the gradual pressure increase behind the RSW. Similar to the experimental  
 113 procedure, IDT was determined using the maximum gradient of the simulated OH time-history profile.



114 The rate coefficients in the UoS sCO<sub>2</sub> 2.0 mechanism were chosen based on a combination of recent  
115 reports, method of determination and how they affected the prediction of 52 IDT datasets [11].

116 A normalized OH sensitivity analysis at the point of ignition was performed to compare the  
117 performances of the two mechanisms and identify the reactions most sensitive to IDT prediction at  
118 different conditions. A positive OH sensitivity coefficient indicates that an increase in the rate of reaction  
119 will reduce IDT (increase reactivity), and vice versa. The performance of the two mechanisms was  
120 compared using Eq. (1), which calculates an average absolute error ( $E$ , %) between the experimental and  
121 simulated IDTs [11].

122 **Eq. (1)** 
$$E(\%) = \frac{1}{N} \sum_{i=1}^N \left| \frac{IDT_{sim,i} - IDT_{exp,i}}{IDT_{exp,i}} \right| \times 100$$

123 Here,  $N$  is the number of data points in a dataset.  $IDT_{sim,i}$  and  $IDT_{exp,i}$  are the simulated and experimental  
124 data points, respectively, for the  $i$ th data point. The average absolute error value is a good way to compare  
125 the mechanism performance across a large number of datasets, where a smaller  $E$  value, ideally within the  
126 experimental uncertainty, indicates a better performance.

127 Only a single modification was made for the creation of UoS sCO<sub>2</sub> 2.0 from the original publication  
128 [11]. The third body efficiency of CO<sub>2</sub> was increased from 2.0 to 3.8 in Reaction 1. This change was found  
129 to lead to large improvements in the performance of the mechanism for this study without adversely  
130 affecting the simulations of datasets used to develop the original mechanism [11]. The importance of  
131 Reaction 1 to H<sub>2</sub> combustion is discussed further in Section 4.



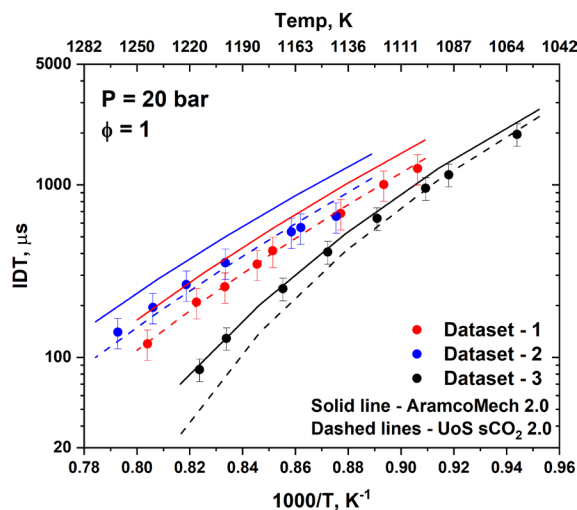
#### 133 **4. Analysis of IDT Datasets**

134 Eight H<sub>2</sub> IDT datasets were measured in this study to allow for mechanism investigation and comparison  
135 over a range of experimental conditions. In the following, discussion and analysis are split in two key  
136 domains. Firstly, the effect of altering CO<sub>2</sub> dilution is considered in Section 4.1, followed by the effect of

137 altering the equivalence ratio in Section 4.2. The results of the quantitative analysis, using Eq. (1), are  
138 presented in Table 1.

#### 139 4.1. Effect of CO<sub>2</sub> Dilution

140 Datasets 1, 2 and 3 investigated IDTs of stoichiometric H<sub>2</sub> in 85% dilution of three different bath gases.  
141 Dataset 1 was composed of 50% CO<sub>2</sub> and 35% N<sub>2</sub>, whilst Datasets 2 and 3 contained 85% CO<sub>2</sub> and 85%  
142 N<sub>2</sub>, respectively. These datasets are shown in Fig. 4 and compared with the predictions of AramcoMech  
143 2.0 and UoS sCO<sub>2</sub> 2.0.



144

145 Fig. 4. Comparison of IDTs of datasets 1 (H<sub>2</sub>:O<sub>2</sub>:N<sub>2</sub>:CO<sub>2</sub>=10:5:35:50), 2 (H<sub>2</sub>:O<sub>2</sub>:CO<sub>2</sub>=10:5:85) and 3  
146 (H<sub>2</sub>:O<sub>2</sub>:N<sub>2</sub>=10:5:85) with AramcoMech 2.0 and UoS sCO<sub>2</sub> 2.0.

147 It may be seen in Fig. 4 that as CO<sub>2</sub> dilution is increased, mixture reactivity is decreased (longer IDTs).  
148 Ignition delays are longer in CO<sub>2</sub> bath gas due to the smaller rate of OH production. This is due to the  
149 branching of H + O<sub>2</sub> reaction between chain propagation (Reaction 1) and chain branching (Reaction 2),  
150 which favours chain propagation for a larger concentration of CO<sub>2</sub>. Additionally, CO<sub>2</sub> consumes H radicals  
151 via the reverse of Reaction 3 to form CO and OH. This reaction competes with Reaction 2 (forward  
152 direction) for H radicals, thus slowing the rate of the branching reaction and reducing the production of  
153 OH radicals. Interestingly, Karimi et al. [16] did not observe any significant difference in IDTs of syngas  
154 in CO<sub>2</sub> vs Ar bath gas.

155       **Reaction 2.**      $\text{H} + \text{O}_2 \rightleftharpoons \text{O} + \text{OH}$

156       **Reaction 3.**      $\text{CO} + \text{OH} \rightleftharpoons \text{CO}_2 + \text{H}$

157       A key observation is the convergence of the three datasets at lower temperatures in Fig. 4. This is not  
158 modelled well by both mechanisms, particularly for datasets 1 and 2. There are two possible explanations  
159 for this. Either the mechanisms lack some chemistry required to model the low-temperature IDTs or the  
160 longest IDT measured for dataset 3 (85%  $\text{CO}_2$ ) suffered from premature ignition because of  
161 inhomogeneities, for example, due to shock bifurcation. Longer IDTs get affected more from bifurcation  
162 as the hot spots associated with bifurcation have enough time to induce localized ignition events [23].  
163 Therefore, for  $\text{CO}_2$  diluted mixtures longer IDTs were limited by the bifurcation growth time scale (500  
164  $\mu\text{s}$ ) as given by Gordon and Ihme [23].

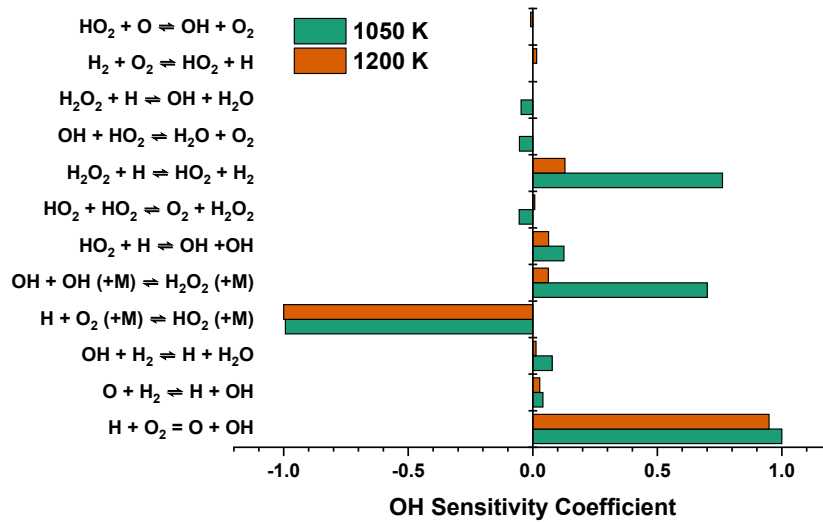
165       Figure 4 and the quantitative analysis in Table 1 show that UoS s $\text{CO}_2$  2.0 gives better predictions for  
166 datasets 1 and 2 which contain  $\text{CO}_2$  dilution, whereas AramcoMech 2.0 performs better for dataset 3 which  
167 only contains  $\text{N}_2$  bath gas. For dataset 3 (85%  $\text{N}_2$ ), whilst both mechanisms predict the four lowest  
168 temperature measurements within the 20% experimental error, UoS s $\text{CO}_2$  2.0 shows a relatively poor  
169 agreement with the three highest temperature data points. To analyze this disagreement, Fig. 5 shows  
170 normalized OH sensitivity analysis of dataset 3 (85%  $\text{N}_2$ ) at 1050 and 1200 K. At the higher temperature  
171 where the agreement is poor, there are only two reactions (Reactions 1 and 2) with a relatively large  
172 sensitivity coefficient. These are the two possible pathways of  $\text{H} + \text{O}_2$  reaction.

173       It is noted that the steep gradient on the predictive curve of dataset 3 is likely due to the temperature  
174 coefficient ( $n$ ) of the rate coefficient of Reaction 2. Even a small alteration of -0.01 had a large effect on  
175 the predictions near the highest temperature data points of datasets 1-3. However, such a change to the  
176 rate coefficient was not made just to fit one dataset. Secondly, Reaction 2 has been investigated thoroughly  
177 by the combustion community [24, 25]. Due to the importance of Reactions 1 and 2 to high-pressure

178 hydrogen and syngas [16] combustion in CO<sub>2</sub>, it is suggested that the rate coefficient of Reaction 1 be  
179 studied in CO<sub>2</sub> bath gas [26, 27] for accurate determination of the third body efficiency of CO<sub>2</sub>.

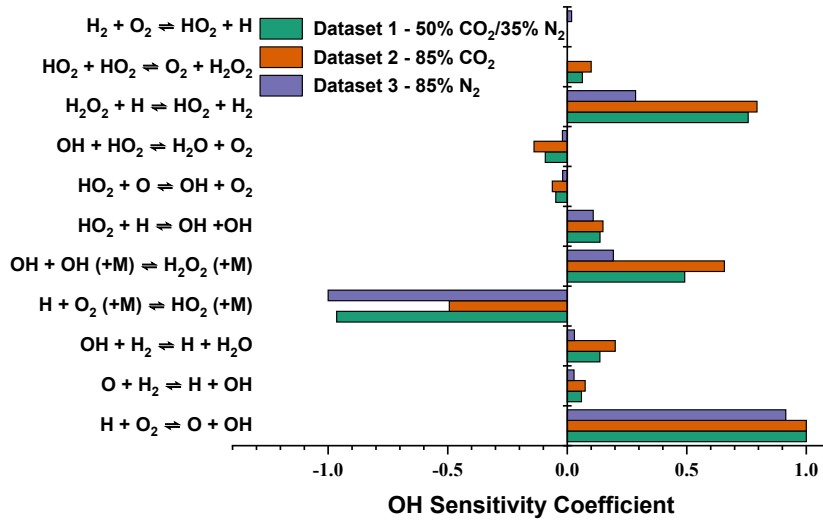
180 Figure 6 compares OH sensitivity analyses of datasets 1-3. A key point to note in Fig. 6 is the greater  
181 similarity of the sensitivity coefficients of 50% CO<sub>2</sub>/ 35% N<sub>2</sub> blend mixture to 85% CO<sub>2</sub> mixture, in  
182 contrast to the sensitivity coefficients of 85% N<sub>2</sub> mixture. Further to this, there is a significant overlap of  
183 the IDTs of datasets 1 and 2 (see Fig. 4) despite a 35% difference in the bath gas composition, and this  
184 trend is predicted by both kinetic mechanisms. The reason for this convergence of IDTs as the  
185 concentration of CO<sub>2</sub> increases is likely due to the chemical effect of CO<sub>2</sub> competing for H radicals via  
186 Reaction 3. This effect is non-linear, and 50% CO<sub>2</sub> leads to a sharp increase in CO mole fraction, whereas  
187 the subsequent 35% addition has a smaller effect on the maximum CO mole fraction and the percentage  
188 of H radicals consumed by Reaction 3 remains similar; therefore, the increase in IDTs isn't as pronounced.

189 These trends suggest that IDT data measured to develop a chemical kinetic mechanism for CO<sub>2</sub>  
190 combustion do not need to be done in 100% CO<sub>2</sub> bath gas. As the controlling reactions and IDTs are  
191 similar for datasets 1 and 2, measuring datasets at only 50% CO<sub>2</sub> produces results that are just as useful  
192 as 85% CO<sub>2</sub>. Reduction in the CO<sub>2</sub> concentration helps in lowering non-ideal effects (e.g., bifurcation), as  
193 discussed in Section 2, which means that IDTs can be measured with smaller uncertainty and at longer  
194 test times. This is not to say that IDT datasets in a pure CO<sub>2</sub> bath gas are not important, but CO<sub>2</sub>/N<sub>2</sub> bath  
195 gas blends provide a useful benchmark with reduced uncertainty in IDT measurements.



196

197 Fig. 5. Normalized OH sensitivity analysis of dataset 3 ( $\text{H}_2:\text{O}_2:\text{N}_2=10:5:85$ ) for UoS sCO<sub>2</sub> 2.0 at 1050 and 1200 K.



198

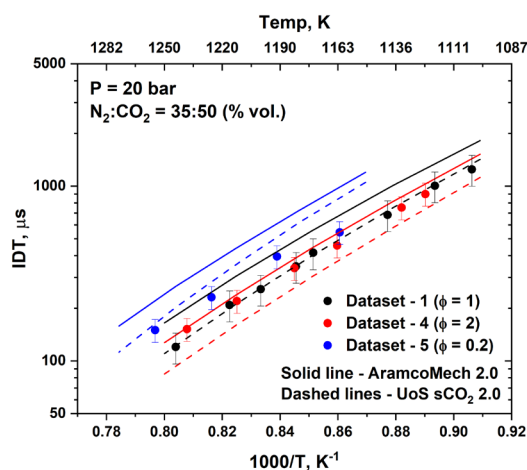
199 Fig. 6. Normalized OH sensitivity analysis of datasets 1 ( $\text{H}_2:\text{O}_2:\text{N}_2:\text{CO}_2=10:5:35:50$ ), 2 ( $\text{H}_2:\text{O}_2:\text{CO}_2=10:5:85$ ) and  
 200 3 ( $\text{H}_2:\text{O}_2:\text{N}_2=10:5:85$ ) for UoS sCO<sub>2</sub> 2.0 at 1150 K.

201 **4.2. Effect of Equivalence Ratio**

202 The effect of altering the equivalence ratio for H<sub>2</sub> ignition was investigated with six datasets. Figure 7  
 203 displays the effect of increasing the equivalence ratio ( $\phi = 0.2, 1, 2$ ) at 20 bar in a bath gas of 50% CO<sub>2</sub> /  
 204 35% N<sub>2</sub>. Datasets 1 and 4 overlap over the entire temperature range, while dataset 5 ( $\phi = 0.2$ ) exhibits  
 205 slightly longer IDTs at high temperatures. These results are consistent with Hu et al. [28] who observed  
 206 a similar overlap of hydrogen IDTs in argon bath gas at 16 bar for  $\phi = 0.5, 1.0$  and 2.0. Sensitivity analysis

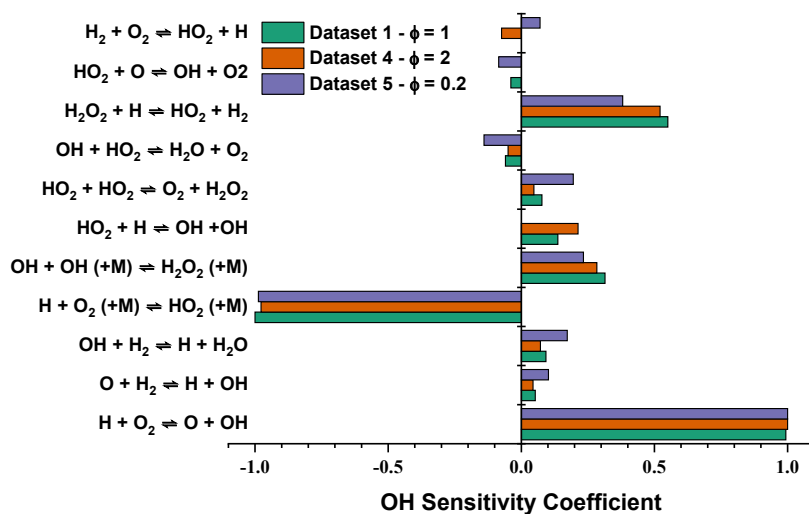
207 in Fig. 8 shows that the three datasets are primarily sensitive to Reactions 1 and 2, and the sensitivity  
 208 coefficients are almost the same for the three equivalence ratios.

209 Table 1 shows that the  $E$  (%) value for dataset 5 ( $\phi = 0.2$ ) is the largest for both AramcoMech 2.0 and  
 210 UoS sCO<sub>2</sub> 2.0 across all H<sub>2</sub> datasets, thus indicating the difficulty to model IDTs at the lowest equivalence  
 211 ratio. Interestingly, the performance of AramcoMech 2.0 improves when moving from  $\phi = 1.0$  to  $\phi = 2.0$ ,  
 212 whereas UoS sCO<sub>2</sub> has better agreement at  $\phi = 1.0$  compared to  $\phi = 2.0$ . This is likely due to the strong  
 213 overlap in Datasets 4 and 5, which is not predicted particularly well by either mechanism.



214

215 Fig. 7. Comparison of IDTs of datasets 1 (H<sub>2</sub>:O<sub>2</sub>:N<sub>2</sub>:CO<sub>2</sub>=10:5:35:50), 4 (H<sub>2</sub>:O<sub>2</sub>:N<sub>2</sub>:CO<sub>2</sub>=12:3:35:50) and 5  
 216 (H<sub>2</sub>:O<sub>2</sub>:N<sub>2</sub>:CO<sub>2</sub>=4.3:10.7:35:50) with AramcoMech 2.0 and UoS sCO<sub>2</sub> 2.0.



217

218 Fig. 8. Normalized OH sensitivity analysis of datasets 1 (H<sub>2</sub>:O<sub>2</sub>:N<sub>2</sub>:CO<sub>2</sub>=10:5:35:50), 4  
 219 (H<sub>2</sub>:O<sub>2</sub>:N<sub>2</sub>:CO<sub>2</sub>=12:3:35:50) and 5 (H<sub>2</sub>:O<sub>2</sub>:N<sub>2</sub>:CO<sub>2</sub>=4.3:10.7:35:50) for UoS sCO<sub>2</sub> 2.0 at 1200 K.

220 Figure 7 shows that UoS sCO<sub>2</sub> 2.0 overpredicts IDTs for dataset 5 ( $\phi = 0.2$ ) while underpredicting dataset  
221 4 ( $\phi = 2.0$ ). Sensitivity analysis (Fig. 8) indicates that one possible explanation is Reaction 4, which has  
222 opposite sensitivity coefficients for  $\phi = 0.2$  and  $\phi = 2.0$ , and it did not appear in the top sensitive reactions  
223 at  $\phi = 1.0$ .

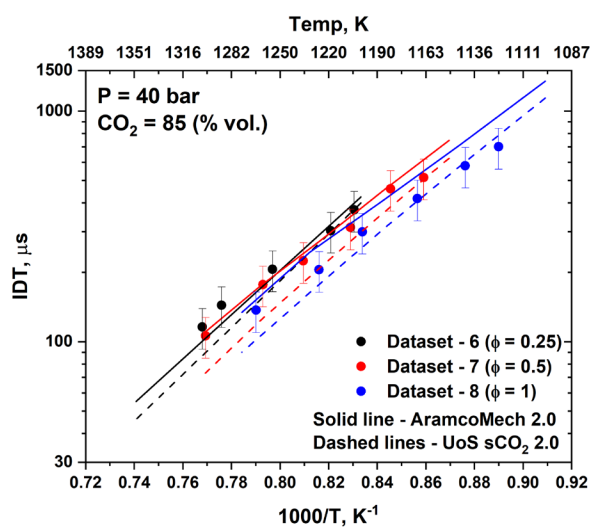


225 While Reaction 5 is the only reaction that has a significantly higher sensitivity at  $\phi = 2.0$  than  $\phi = 0.2$ ,  
226 Reactions 6, 7 and 8 have a much larger sensitivity coefficient at  $\phi = 0.2$ . It may be anticipated that tuning  
227 the rate coefficients of these reactions will reduce the effect of equivalence ratio changes on simulated  
228 IDTs, and thus lead to the mechanism predictions being in better agreement with the experimental IDTs.  
229 This is proposed as one of the possible future routes for mechanism optimization. Nonetheless, it must be  
230 noted that except for dataset 4, UoS sCO<sub>2</sub> 2.0 significantly outperformed AramcoMech 2.0 in predicting  
231 the equivalence ratio dependence.



236 Figure 9 shows the effect of increasing the equivalence ratio ( $\phi = 0.25, 0.5, 1$ ) in 85% CO<sub>2</sub> bath gas for  
237 H<sub>2</sub> ignition at 40 bar. In comparison to 20 bar (Fig. 7), the performance of AramcoMech 2.0 is much more  
238 competitive. This is surprising as the mechanism was originally validated for relatively low pressures and  
239 low CO<sub>2</sub> dilutions. The performance of UoS sCO<sub>2</sub> 2.0 is also better at 40 bar than 20 bar. This is likely  
240 because the mechanism was primarily validated using three H<sub>2</sub> IDT datasets of Shao et al. [29], where the  
241 lowest pressure was ~40 bar with CO<sub>2</sub> dilution of 85% (which is directly comparable with dataset 6 from  
242 the current work). This means that UoS sCO<sub>2</sub> 2.0 was not validated to model H<sub>2</sub> IDTs below 40 bar. This  
243 illustrates the importance of the IDT data reported here in developing a comprehensive chemical kinetic

244 mechanism for modelling sCO<sub>2</sub> combustion. While datasets 6, 7 and 8 shown in Fig. 9 are not directly  
 245 comparable to those at 20 bar (Fig. 7) due to the different bath gas composition, the trends observed are  
 246 very similar. Although the equivalence ratio range is smaller for the three datasets at 40 bar compared to  
 247 those at 20 bar, there is a large overlap of IDTs (Fig. 9) at the three equivalence ratios with dataset 8 ( $\phi =$   
 248 1.0) being slightly faster. AramcoMech predicts negligible equivalence ratio dependence while UoS sCO<sub>2</sub>  
 249 predicts a small variation of IDTs with equivalence ratio which is more aligned with the experimental  
 250 data.



251

252 Fig. 9. Comparison of IDTs of datasets 6 (H<sub>2</sub>:O<sub>2</sub>:CO<sub>2</sub>=5:10:85), 7 (H<sub>2</sub>:O<sub>2</sub>:CO<sub>2</sub>=7.5:7.5:85) and 8  
 253 (H<sub>2</sub>:O<sub>2</sub>:CO<sub>2</sub>=10:5:85) with AramcoMech 2.0 and UoS sCO<sub>2</sub> 2.0.

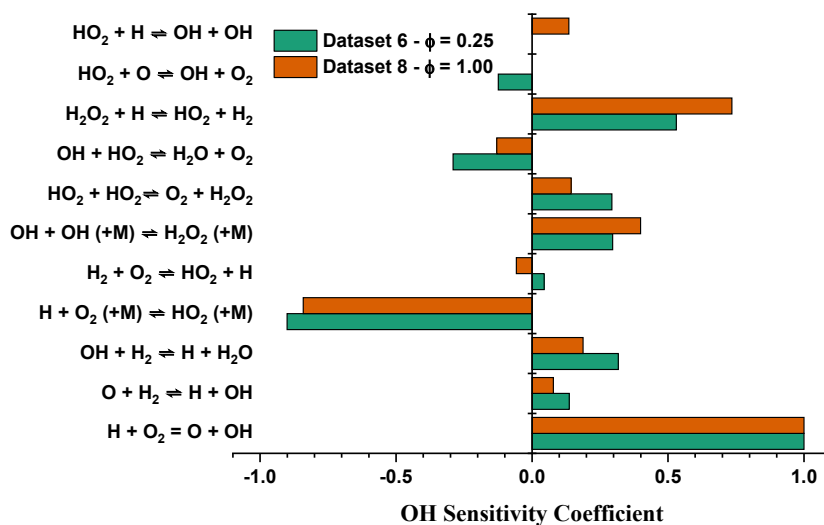
254 Figure 10 shows normalized OH sensitivity analysis of datasets 6 and 8 at 1250 K, which is used to  
 255 visualize the effect of equivalence ratio on H<sub>2</sub> ignition at 40 bar. In Fig. 9, UoS sCO<sub>2</sub> 2.0 predicts faster  
 256 IDTs compared to the experiments at high temperatures. This is likely due to the temperature dependence  
 257 of Reaction 2, as discussed earlier. Another possible explanation is the overprediction of the rate  
 258 coefficient of Reaction 9 which has the second-largest positive sensitivity coefficient in Fig. 10.  
 259 AramcoMech 2.0 and UoS sCO<sub>2</sub> 2.0 both use the rate coefficient of Reaction 9 from Ellingson et al. [30],  
 260 with UoS sCO<sub>2</sub> 2.0 having a slightly smaller *A* factor, reduced within the experimental uncertainty [11].  
 261 Therefore, there may be a significant effect on the predicted IDTs if the rate coefficient of Reaction 9 was



262 changed to those given by Tsang and Hampson [31] or Wu et al. [32], where both of these studies propose  
 263 a smaller A factor but a larger temperature coefficient.

264 **Reaction 9.**  $\text{H}_2\text{O}_2 + \text{H} \rightleftharpoons \text{HO}_2 + \text{H}_2$

265 Further experiments at the high and low-temperature ends would be helpful in understanding these  
 266 discrepancies. Longer test times can be achieved with driver gas tailoring in a shock tube [33] but could  
 267 be more prone to non-ideal effects. Experiments at shorter test times are challenging due to the larger  
 268 uncertainty in shock tube measurements below 100  $\mu\text{s}$ .



269

270 Fig. 10. Normalized OH sensitivity analysis of datasets 6 ( $\text{H}_2:\text{O}_2:\text{CO}_2=5:10:85$ ) and 8 ( $\text{H}_2:\text{O}_2:\text{CO}_2=10:5:85$ ) for  
 271 UoS sCO<sub>2</sub> 2.0 at 1250 K.

## 272 5. Validation of UoS sCO<sub>2</sub> Mechanism

273 A key objective of this study is to validate UoS sCO<sub>2</sub> 2.0 for predicting IDTs of H<sub>2</sub> in CO<sub>2</sub> bath gas. For  
 274 the eight H<sub>2</sub> datasets studied here, the average absolute error ( $E$ ) was determined to be 16.1% for UoS  
 275 sCO<sub>2</sub> 2.0, which is a significant improvement compared to 28.1% of AramcoMech 2.0. In addition, UoS  
 276 sCO<sub>2</sub> 2.0 fits six datasets within a 20% error, which is the typical uncertainty for shock tube IDT  
 277 measurements. UoS cCO<sub>2</sub> mechanism, which was initially developed using limited H<sub>2</sub> IDT data,  
 278 significantly outperforms AramcoMech 2.0, a well-validated chemical kinetic mechanism across a range  
 279 of conditions. The current work validates the performance of the UoS sCO<sub>2</sub> 2.0 mechanism across a range

280 of equivalence ratios, pressures, and bath gas compositions for CO<sub>2</sub>-diluted H<sub>2</sub> ignition. This work also  
281 identifies areas of improvement for prediction H<sub>2</sub> ignition in CO<sub>2</sub> bath gas. This includes measuring the  
282 reaction rate coefficient of Reaction 1 in CO<sub>2</sub> bath gas and IDT measurements at lower temperatures.  
283 Another suggestion is to measure OH time-histories for H<sub>2</sub> combustion in CO<sub>2</sub> to validate the mechanisms'  
284 ability in modelling the concentration of the most important radical of H<sub>2</sub> combustion.

## 285 **6. Conclusions**

286 The present study investigates the combustion behaviour of H<sub>2</sub> in CO<sub>2</sub> bath gas by performing IDT  
287 measurements of H<sub>2</sub> for various equivalence ratios and bath gas compositions at 20 and 40 bar. These data  
288 fill the gaps in literature on experimental work of hydrogen IDTs in CO<sub>2</sub>. Measured IDT data were used  
289 to validate the UoS sCO<sub>2</sub> 2.0 chemical kinetic mechanism which was developed recently to model the  
290 combustion of methane, H<sub>2</sub>, and syngas in CO<sub>2</sub> bath gas. UoS sCO<sub>2</sub> 2.0 outperformed AramcoMech 2.0  
291 in simulating IDT datasets as evaluated quantitatively by comparing the average percentage difference  
292 between the experimental and simulated IDTs. While there is still room for mechanism improvement as  
293 identified by the sensitivity analysis and discussed in the present study, these data coupled with previous  
294 works provide a wide-ranging validation platform for mechanisms to model IDTs of H<sub>2</sub> in CO<sub>2</sub> bath gas  
295 over a wide range of conditions.

## 296 **Acknowledgements**

297 The work of KAUST authors was funded by baseline research funds at King Abdullah University of  
298 Science and Technology (KAUST). The work of UoS was supported by EPSRC Centre for Doctoral  
299 Training in Resilient Decarbonised Fuel Energy Systems (Grant number: EP/S022996/1) and the  
300 International Flame Research Federation (IFRF).

## 301 **Supplementary Material**

302 This work contains supplementary material.

303 (Uncertainty of measured IDTs, Tables of measured IDTs, Mechanism files of UoS sCO<sub>2</sub> 2.0).

## 304 References

- 305  
306 [1] V. Masson-Delmotte, P. Zhai, A. Pirani, S.L., Connors, C. Péan, S. Berger, N. Caud, Y. Chen, L. Goldfarb, M.I. Gomis, M. Huang, K. Leitzell, E. Lonnoy,  
307 J.B.R., Matthews, T.K. Maycock, T. Waterfield, O. Yelekçi, R. Yu, B. Zhou, IPCC, 2021: Climate Change 2021: The Physical Science Basis. Contribution of  
308 Working Group I to the Sixth Assessment Report of the Intergovernmental Panel on Climate Change, 2021.
- 309 [2] K.L. Ebi, J. Vanos, J.W. Baldwin, J.E. Bell, D.M. Hondula, N.A. Errett, K. Hayes, C.E. Reid, S. Saha, J. Spector, P. Berry, Extreme Weather and Climate  
310 Change: Population Health and Health System Implications, *Annual Review of Public Health* 42 (2021) 293-315.
- 311 [3] N. Höhne, M.J. Gidden, M. den Elzen, F. Hans, C. Fyson, A. Geiges, M.L. Jeffery, S. Gonzales-Zuñiga, S. Mooldijk, W. Hare, J. Rogelj, Wave of net zero  
312 emission targets opens window to meeting the Paris Agreement, *Nature Climate Change* (2021).
- 313 [4] R.J. Allam, M.R. Palmer, G.W. Brown, J. Fetvedt, D. Freed, H. Nomoto, M. Itoh, N. Okita, C. Jones, High efficiency and low cost of electricity generation  
314 from fossil fuels while eliminating atmospheric emissions, including carbon dioxide, *GHGT-11* 37 (2013) 1135-1149.
- 315 [5] NetPower, Home. <https://www.netpower.com/> (accessed 7th November 2019).
- 316 [6] A. Rathi, U.S. startup plans to build first zero-emission gas power plants. [https://www.bloomberg.com/news/articles/2021-04-15/u-s-startup-plans-to-build-](https://www.bloomberg.com/news/articles/2021-04-15/u-s-startup-plans-to-build-first-zero-emission-gas-power-plants)  
317 [first-zero-emission-gas-power-plants](https://www.bloomberg.com/news/articles/2021-04-15/u-s-startup-plans-to-build-first-zero-emission-gas-power-plants) (accessed 15th April 2021).
- 318 [7] G. Kelsall, 8 Rivers Capital and Sembcorp Energy UK's first zero emissions power plant. [https://ifrf.net/ifrf-blog/8-rivers-capital-and-semcorp-energy-](https://ifrf.net/ifrf-blog/8-rivers-capital-and-semcorp-energy-uk-to-develop-uks-first-net-zero-emissions-power-plant/)  
319 [uk-to-develop-uks-first-net-zero-emissions-power-plant/](https://ifrf.net/ifrf-blog/8-rivers-capital-and-semcorp-energy-uk-to-develop-uks-first-net-zero-emissions-power-plant/) (accessed 2nd August 2021).
- 320 [8] R.J. Allam, J.E. Fetvedt, B.A. Forrest, D.A. Freed, The oxy-fuel, supercritical CO<sub>2</sub> Allam cycle: new cycle developments to produce even lower-cost  
321 electricity from fossil fuels without atmospheric emissions, *Proceedings of the ASME Turbo Expo: Turbine Technical Conference and Exposition* 3b (2014).
- 322 [9] J.M. Harman-Thomas, M. Pourkashanian, K.J. Hughes, The chemical kinetic mechanism for combustion in supercritical carbon dioxide, 4th European  
323 sCO<sub>2</sub> Conference for Energy Systems, Online, 2021, pp. 28-37.
- 324 [10] J.K. Shao, R. Choudhary, D.E. Davidson, R.K. Hanson, S. Barak, S. Vasu, Ignition delay times of methane and hydrogen highly diluted in carbon dioxide  
325 at high pressures up to 300 atm, *Proceedings of the Combustion Institute* 37 (2019) 4555-4562.
- 326 [11] J. Harman-Thomas, K.J. Hughes, M. Pourkashanian, The development of a chemical kinetic mechanism for combustion in supercritical carbon dioxide,  
327 *Energy* (2022) 124490.
- 328 [12] M. Alabbad, Y. Li, K. AlJohani, G. Kenny, K. Hakimov, M. Al-lehaibi, A.-H. Emwas, P. Meier, J. Badra, H. Curran, Ignition delay time measurements  
329 of diesel and gasoline blends, *Combustion and Flame* 222 (2020) 460-475.
- 330 [13] M. Alabbad, T. Javed, F. Khaled, J. Badra, A. Farooq, Ignition delay time measurements of primary reference fuel blends, *Combustion and Flame* 178  
331 (2017) 205-216.
- 332 [14] A.S. AlRamadan, J. Badra, T. Javed, M. Al-Abbad, N. Bokhumseen, P. Gaillard, H. Babiker, A. Farooq, S.M. Sarathy, Mixed butanols addition to gasoline  
333 surrogates: Shock tube ignition delay time measurements and chemical kinetic modeling, *Combustion and Flame* 162 (2015) 3971-3979.
- 334 [15] J.W. Hargis, E.L. Petersen, Methane ignition in a shock tube with high levels of CO<sub>2</sub> dilution: consideration of the reflected-shock bifurcation, *Energy &*  
335 *Fuels* 29 (2015) 7712-7726.
- 336 [16] M. Karimi, B. Ochs, W. Sun, D. Ranjan, High pressure ignition delay times of H<sub>2</sub>/CO mixture in carbon dioxide and argon diluent, *Proceedings of the*  
337 *Combustion Institute* (2020).
- 338 [17] H. Mark, The interaction of a reflected shock wave with the boundary layer in a shock tube, Cornell University, Ithaca, New York, United States, 1958.
- 339 [18] D. Bull, D. Edwards, An investigation of the reflected shock interaction process in a shock tube, *AIAA Journal* 6 (1968) 1549-1555.
- 340 [19] H. Kleine, V. Lyakhov, L. Gvozdeva, H. Grönig, Bifurcation of a reflected shock wave in a shock tube, *Shock Waves*, Springer 1992, pp. 261-266.
- 341 [20] E.L. Petersen, Interpreting endwall and sidewall measurements in shock-tube ignition studies, *Combustion Science and Technology* 181 (2009) 1123-  
342 1144.
- 343 [21] M. Lamnaouer, A. Kassab, E. Divo, N. Polley, R. Garza-Urquiza, E. Petersen, A conjugate axisymmetric model of a high-pressure shock-tube facility,  
344 *International Journal of Numerical Methods for Heat & Fluid Flow* (2014).
- 345 [22] W.K. Metcalfe, S.M. Burke, S.S. Ahmed, H.J. Curran, A hierarchical and comparative kinetic modeling study of C1 – C2 hydrocarbon and oxygenated  
346 fuels, *International Journal of Chemical Kinetics* 45 (2013) 638-675.
- 347 [23] K.P. Grogan, M. Ihme, Regimes describing shock boundary layer interaction and ignition in shock tubes, *Proceedings of the Combustion Institute* 36  
348 (2017) 2927-2935.
- 349 [24] Z. Hong, D.F. Davidson, E.A. Barbour, R.K. Hanson, A new shock tube study of the H + O<sub>2</sub> → OH + O reaction rate using tunable diode laser absorption  
350 of H<sub>2</sub>O near 2.5 μm, *Proceedings of the Combustion Institute* 33 (2011) 309-316.
- 351 [25] S. Wang, D.F. Davidson, R.K. Hanson, Shock Tube and Laser Absorption Study of CH<sub>2</sub>O Oxidation via Simultaneous Measurements of OH and CO,  
352 *The Journal of Physical Chemistry A* 121 (2017) 8561-8568.
- 353 [26] J. Shao, Shock tube studies of hydrocarbon fuels at elevated pressures, Mechanical Engineering, Stanford University, Stanford, 2019.
- 354 [27] S.S. Vasu, D.F. Davidson, R.K. Hanson, Shock tube study of syngas ignition in rich CO<sub>2</sub> mixtures and determination of the rate of H+O<sub>2</sub>+ CO<sub>2</sub> →  
355 HO<sub>2</sub>+CO<sub>2</sub>, *Energy & Fuels* 25 (2011) 990-997.
- 356 [28] E. Hu, L. Pan, Z. Gao, X. Lu, X. Meng, Z. Huang, Shock tube study on ignition delay of hydrogen and evaluation of various kinetic models, *International*  
357 *Journal of Hydrogen Energy* 41 (2016) 13261-13280.
- 358 [29] J. Shao, R. Choudhary, D.F. Davidson, R.K. Hanson, S. Barak, S. Vasu, Ignition delay times of methane and hydrogen highly diluted in carbon dioxide  
359 at high pressures up to 300 atm, *Proceedings of the Combustion Institute* 37 (2019) 4555-4562.
- 360 [30] B.A. Ellingson, D.P. Theis, O. Tishchenko, J. Zheng, D.G. Truhlar, Reactions of hydrogen atom with hydrogen peroxide, *The Journal of Physical*  
361 *Chemistry A* 111 (2007) 13554-13566.
- 362 [31] W. Tsang, R.F. Hampson, Chemical kinetic data base for combustion chemistry. Part I. Methane and related compounds, *Journal of Physical and Chemical*  
363 *Reference Data* 15 (1986) 1087-1279.
- 364 [32] Y. Wu, S. Panigrahy, A.B. Sahu, C. Bariki, J. Beeckmann, J. Liang, A.A. Mohamed, S. Dong, C. Tang, H. Pitsch, Understanding the antagonistic effect  
365 of methanol as a component in surrogate fuel models: A case study of methanol/n-heptane mixtures, *Combustion and Flame* 226 (2021) 229-242.
- 366 [33] M.F. Campbell, T. Parise, A.M. Tulgestke, R.M. Spearrin, D.F. Davidson, R.K. Hanson, Strategies for obtaining long constant-pressure test times in  
367 shock tubes, *Shock Waves* 25 (2015) 651-665.

368